Influence of skin type and laser wavelength on laser-evoked potentials

Frahm, Ken Steffen; Gervasio, Sabata; Arguissain, Federico; Mouraux, André

Published in:
European Journal of Pain

DOI (link to publication from Publisher):
10.1002/ejp.2152

Publication date:
2023

Document Version
Publisher's PDF, also known as Version of record

Received: 12 January 2023 | Revised: 3 May 2023 | Accepted: 8 June 2023

DOI: 10.1002/ejp.2152

EJP European Journal of Pain

ORIGINAL ARTICLE

Influence of skin type and laser wavelength on laser-evoked potentials

Ken Steffen Frahm[1] | **Sabata Gervasio**[2] | **Federico Arguissain**[1] | **André Mouraux**[3]

[1]Integrative Neuroscience Group, CNAP – Center for Neuroplasticity and Pain, SMI©, Department of Health Science & Technology, Aalborg University, Aalborg, Denmark

[2]Neural Engineering and Neurophysiology Group, SMI©, Department of Health Science & Technology, Aalborg University, Aalborg, Denmark

[3]Université Catholique de Louvain, Institute of Neuroscience (IoNS), Faculty of Medicine, Bruxelles, Belgium

Correspondence
Ken Steffen Frahm, Integrative Neuroscience Group, CNAP – Center for Neuroplasticity and Pain, SMI©, Department of Health Science & Technology, Aalborg University, Aalborg, Denmark.
Email: ksf@hst.aau.dk

Funding information
Danish National Research Foundation, Grant/Award Number: DNRF121

Abstract

Background: Infrared laser stimulation is a valuable tool in pain research, its primary application being the recording of laser-evoked brain potentials (LEPs). Different types of laser stimulators, varying in their skin penetrance, are likely to have a large influence on the LEPs, when stimulating different skin types. The aim of this study was to investigate how LEPs depend on laser type and skin location.

Methods: Two different laser stimulators (CO_2 and Nd:YAP) were used to compare LEPs in healthy subjects. Stimuli were delivered to the hand dorsum and palm to investigate the effects of skin type on the evoked responses. Stimulus-evoked brain responses were recorded using EEG and perceived intensity ratings were recorded. Computational modelling was used to investigate the observed differences.

Results: LEPs evoked by stimulation of the hairy skin were similar between CO_2 and Nd:YAP stimulation. In contrast, LEPs elicited from the palm were markedly different and barely present for CO_2 stimulation. There was a significant interaction between laser type and skin type (RM-ANOVA, $p < 0.05$) likely due to smaller CO_2 LEPs in the palm. CO_2 stimuli to the palm also elicited significantly lower perceived intensities. The computational model showed that the observed differences were explainable by the laser absorption characteristics and skin thickness affecting the temperature profile at the dermo-epidermal junction (DEJ).

Conclusions: This study shows that LEP elicitation depends on the combination of laser penetrance and skin type. Low penetrance stimuli, from a CO_2 laser, elicited significantly lower LEPs and perceived intensities in the palm.

Significance: This study showed that the elicitation of laser-evoked potentials in healthy humans greatly depends on the combination of laser stimulator type and skin type. It was shown that high penetrance laser stimuli are capable of eliciting responses in both hairy and glabrous skin, whereas low penetrance stimuli barely elicited responses from the glabrous skin. Computational modelling was used to

demonstrate that the results could be fully explained by the combination of laser type and skin thickness.

1 | INTRODUCTION

Cutaneous laser stimulation has been used in pain research for nearly half a century (Mor & Carmon, 1975). The overriding advantage of laser stimulation is the ability to deliver stimuli that can reliably activate heat-sensitive nociceptors in the skin in a phasic fashion, without skin contact and thus without co-activation of non-nociceptive afferents.

Historically, the most used laser technology is the CO_2 laser (Cruccu et al., 2008; Plaghki & Mouraux, 2003). Some research labs have developed CO_2 lasers with advanced temperature-controlled systems (Churyukanov et al., 2012; Meyer et al., 1976), which allow highly repeatable stimulation and contributed to significantly advancing our understanding of the thermosensitive nociceptive system (Churyukanov et al., 2012; Treede et al., 1995). Besides temperature control, CO_2 lasers have been combined with scanner head technology to allow the investigation of complex temporospatial phenomena in the pain system such as two-point discrimination (Frahm & Gervasio, 2021), graphestesia (Mørch et al., 2010) and directional discrimination (Frahm et al., 2018). Over time, different laser technologies have emerged and found their way into pain research. Another type of laser, whose use in pain research has increased in recent decades, is the solid-state laser such as the Nd:YAP (neodymium-doped yttrium aluminium perovskite) laser (Iannetti et al., 2006; Perchet et al., 2008). The underlying technology of the laser (gas, solid-state, diode, etc.) defines the wavelength of the emitted laser photon. These wavelengths dictate how the radiation energy from the laser photons is absorbed and converted into heat within the skin (Cruccu et al., 2008; Jacques, 1996, 2013). CO_2 lasers are in the far infrared spectrum (10.6 μm) and its radiation is absorbed in the water molecules of the skin, whereas visual and near-infrared wavelengths, such as argon, diode, Nd:YAP and thulium lasers, are primarily absorbed in the melanin of the skin. The different absorption profiles cause the heat distribution to vary significantly. These differences affect how the heat-sensitive afferents are activated.

Laser stimuli can be used to investigate the nociceptive system both using psychophysical parameters, such as warm and pain detection thresholds, and intensity ratings or reaction times to supra-threshold responses. Electroencephalography (EEG) has been used to record brain responses to laser stimuli, referred to as laser-evoked potentials (LEPs). LEPs have been studied extensively in both patients and healthy subjects, and are recommended by the EFNS (European Federation of Neurological Societies) to investigate the function of nociceptive pathways in patients, including those suffering from neuropathic pain (Cruccu et al., 2010). Following cutaneous laser stimuli, the most robust deflection in the EEG signal is the N2P2 complex, which is largest at the vertex (Cz). This deflection is believed to originate bilaterally from the operculo-insular cortex, as well as from the anterior cingulate gyrus (Garcia-Larrea et al., 2003; Valeriani et al., 2012). The N2P2 complex, is preceded by a smaller component, named the N1, which can be recorded in the central-temporal areas contralateral to the stimulus when stimulating the hand (Valeriani et al., 2012). This N1 peak is typically less robust than the N2P2 (Iannetti et al., 2006; Truini et al., 2005).

CO_2 laser stimuli are absorbed very superficially, meaning that the heat needs to be passively conducted from the more superficial tissue to where the nociceptors terminate, typically around the dermo-epidermal junction (DEJ) (Frahm et al., 2010). This passive conduction will affect the synchronization of the afferent volley and therefore the LEPs. CO_2 laser stimuli are generally forced to have longer durations than solid-state laser stimuli because, despite being capable of delivering stimuli as short as 1 ms or shorter, the laser power would have to be very high to deliver sufficient energy to activate the deeper terminating afferents. Such high-power stimuli would likely burn the skin as the surface temperature would exceed the thermal damage threshold. In contrast, the Nd:YAP laser penetrates deeper and creates a more uniform temperature across various tissue depths, including those where the afferents terminate, thus eliminating the need for passive heat conduction in the tissue to activate the afferents. Once the temperature at the afferent terminals is sufficiently high, action potentials are initiated.

Since Nd:YAP laser stimuli penetrate deeper than CO_2 laser stimuli, one might speculate whether the afferent population being activated is the same for both laser types. A study by Perchet et al. showed that LEPs from Nd:YAP and CO_2 lasers are comparable, but LEPs by Nd:YAP stimuli have shorter latencies and larger amplitudes (Perchet et al., 2008). The authors attributed these findings to differences in the stimulation characteristics. Additionally, studies using capsaicin deafferentation have shown that LEPs are reduced from both Nd:YAP laser stimuli (La Cesa et al., 2018) and CO_2 laser stimuli (Mouraux et al., 2010). Both of these studies only investigated LEPs from the hairy skin, and indicate that the heat-sensitive afferents activated by Nd:YAP and CO_2 laser stimuli appear similar, at least in hairy skin.

To our knowledge, no studies have yet compared the LEPs elicited by low-penetrance and high-penetrance laser stimulation across different skin types and stimulation intensities. Further insights into how the combination of these stimulus characteristics affect LEPs are needed to understand the effect each parameter has on the nociceptor activation. Previous research has shown how computational modelling can improve our understanding of cutaneous laser stimuli (Bromm & Treede, 1983; Frahm et al., 2010, 2020; Haimi-Cohen et al., 1983; Lejeune et al., 2023; Marchandise et al., 2014). One important advantage of such models is the ability to simulate intracutaneous temperatures, which govern the activation of heat-sensitive afferents. It is, therefore, possible to investigate how different stimulus combinations can activate skin afferents and do so without placing temperature probes which inherently affect the thermodynamic properties of the tissue and likely the activation of the sensory afferents. Recently, we have investigated how the perception of laser stimulation depends on the combination of laser type and skin location (Frahm et al., 2020). In that study, we developed and experimentally validated a computational model, which allows investigating laser stimuli applied to different skin locations and with different laser types.

The aim of the present study was to investigate how evoked potentials following both low (CO_2) and high (Nd:YAP) penetrance laser stimuli depend on the stimulation site, namely hairy or glabrous skin of the hand palm, and if computational modelling of the combination of skin anatomy and stimulation characteristics can explain observed differences in the evoked responses.

2 | METHODS

2.1 | Participants

Thirteen healthy Caucasian subjects participated in this study (6 females, mean age 29 ± 4 years). All participants gave oral and written informed consent before the experiment started. The Helsinki Declaration was respected. The experiment was approved by the local ethical committee. During the experiment, the subjects laid in a bed with a raised headrest and were stimulated at the right hand. The experiments were conducted in a temperature-controlled room (21 ± 1°C).

2.2 | Laser stimulation

Two different laser stimulators were used to deliver the stimuli, (1) an Nd:YAP laser (El:EN, DEKA) with a wavelength of 1.34 μm and a beam width of 4 mm ($1/e^2$, Gaussian), and (2) a CO_2 laser (Synrad Firestar ti-series, Synrad) with a wavelength of 10.6 μm and a beam width of 5.7 mm ($1/e^2$, Gaussian). For both lasers, two different intensities were used, one close to the approximate pain threshold and the other above pain threshold (Frahm et al., 2020). For the Nd:YAP laser, intensities of 4 and 4.5 J (200 and 225 W, 20 ms duration) were used, corresponding to 31.8 and 35.8 J/cm^2 respectively. For the CO_2 laser, intensities of 0.96 and 1.12 J (4.8 and 5.6 W, 200 ms duration) were used, corresponding to 3.8 and 4.4 J/cm^2 respectively. The stimulation parameters were based on our previous study as the two intensities were expected to be perceived at around pain threshold and slightly above pain threshold when stimulating the hairy skin of the hand dorsum (Frahm et al., 2020). The same laser stimulation intensities were used both for the dorsum and palm of the hand. During the laser stimuli, it was ensured that the laser beam was perpendicular to the irradiated skin area. The stimulation site was changed slightly after each stimulus.

2.3 | EEG recordings

The electrical brain activity during laser stimulation was recorded using electroencephalography (EEG). The EEG was recorded using a 32-channel setup based on the international 10–20 system. The left earlobe was used as reference and AFz served as the ground. The electrodes were active, that is, with a preamplification occurring at each electrode location to reduce contamination by environmental noise (gtec). The electrode impedance was kept below 30 kΩ. The data were sampled using a g.HIAMP amplifier (gtec), with a sampling frequency of 1200 Hz and a 24-bit resolution.

2.4 | Experimental protocol

The experiment was divided into eight blocks. Within each block, the same combination of laser type, intensity and stimulation site (dorsum or palm) was delivered. A total of 30 stimuli were delivered in each block. Between each stimulus, there was a 15–30 s pause. A 2-min break was held after 15 stimulations in each block. The combination of laser type, skin site and stimulation intensity was randomized for each subject. Subjects had a 5 min break between blocks.

To measure the reaction times (RT), subjects were asked to press a button as soon as the stimulation was perceived. After pushing the button, the subjects had to indicate the perceived intensity on a numerical rating scale

(NRS) anchored as 0: no perception, 3: pain threshold, 10: maximum imaginable pain. This scale was used as it was expected that the perceived intensities would be both below and above the pain threshold (Frahm et al., 2020; Madden et al., 2019).

2.5 | Computational modelling of cutaneous laser stimuli

The computational model developed and validated in our previous study (Frahm et al., 2020) was used in this study to investigate how the experimental results (primarily the LEPs) depended on the combination of laser type and skin type. The model was based on the Finite Element Method and implemented in COMSOL Multiphysics 5.4 (COMSOLA/S), using a 2D-axial symmetry. The model consisted of three tissue compartments representing the stratum corneum, the vital epidermis and the dermis. The model parameters are reported in Table 1. The model was experimentally validated using thermographic data from laser stimulation in healthy human subjects. To allow sufficient thermographic data for model validation, relative long stimulation durations, nevertheless considered to be in the range used for LEP recordings' range, were used to validate the model (20 ms for Nd:YAP and 200 ms for CO_2). The initial tissue temperature in the model was set to 35°C. See Frahm et al., 2020 for more details on the model implementation. The model was used to simulate the same combinations of laser wavelength, skin type and stimulation intensities that were used experimentally. For each condition, the maximum nociceptor temperature, defined as the DEJ temperature; and the tissue volume in the vital epidermis and dermis, reaching a temperature above Aδ nociceptor threshold (46°C, (Churyukanov et al., 2012)) were extracted. These values were then compared to the experimental results (LEPs).

Additionally, the existing model was updated to simulate shorter CO_2 laser durations, similar to those of the Nd:YAP stimulation, that is, 20 ms. The 20-ms duration was used for two stimulation situations, (1) a 20-ms CO_2 stimulation reaching a similar surface temperature to the one used experimentally in this study, and (2) a 20-ms CO_2 stimulation reaching a similar nociceptor temperature (DEJ) to that of the experimental stimulus used in this study. For the hairy skin, the laser power for the CO_2 laser had to be increased to 20.25 W to reach the same surface temperature after 20 ms, and to 36.0 W to reach the same DEJ temperature. For the glabrous skin in the palm, the CO_2 laser power had to be increased to 22.8 and 52.5 W respectively.

2.6 | Data analysis and statistics

2.6.1 | EEG analysis

The EEG data were analysed offline using EEGlab (Delorme & Makeig, 2004) on Matlab R2021a (Mathwork). The EEG was bandpass filtered between 2 and 50 Hz (Butterworth, 4th order). Epochs were extracted based on onset of laser stimulation and segmented from 500 ms before onset to 1 s following onset. Artefacts were removed using artefact subspace reconstruction (Chang et al., 2020). Data were further processed using independent component analysis to remove artefacts. The epochs were baseline-corrected (baseline: 500 ms before stimulation onset). Epochs with amplitude exceeding ±100 μV were removed. Finally, epochs were averaged across subjects and conditions. The N2P2 complex was extracted from the Cz channel, re-referenced to the average reference. Due to the different stimulation duration of the two laser types, the window to determine the LEP components was adjusted differently for each laser type. For the Nd:YAP, the N2 was

TABLE 1 Model parameter used in the computational model of the laser stimulation.

	Thermal parameters	Optical parameters	Thickness
Stratum corneum	k: 0.3 W (m·K) c: 1200 kg/m^3 ρ: 3600 J/(kg·k)	μ_a Nd:YAP: 150 m^{-1} μ_a CO_2: 20,000 m^{-1}	Dorsum: 20 μm Palm: 30 μm
Vital Epidermis	k: 0.35 W (m·K) c: 1200 kg/m^3 ρ: 3600 J/(kg·k)	μ_a Nd:YAP: 225 m^{-1} μ_a CO_2: 75,000 m^{-1}	Dorsum: 30 μm Palm: 100 μm
Dermis	k: 0.6 W (m·K) c: 1200 kg/m^3 ρ: 3800 J/(kg·k)	μ_a Nd:YAP: 350 m^{-1} μ_a CO_2: 100,000 m^{-1}	1300 μm

Note: Thermal parameters include thermal conductivity, k, specific heat, c and density, ρ. The optical parameter include the absorption coefficient, μ_a and varied with laser type. Tissue thicknesses varied with skin type, the palm had thicker stratum corneum and vital epidermis.

extracted in the 150–350 ms window, while for CO_2 the window used was 350–550 ms. For the P2, the Nd:YAP window used was 250–500 ms and for CO_2 the window was 450–650 ms. The N1 peak was extracted from T7 re-referenced to Fz. The window used to the calculation of N1 was 100–300 ms for the Nd:YAP laser and 300–500 for the CO_2 laser.

2.6.2 | Statistical analysis

Both the reaction times and NRS data were analysed using a three-way repeated measures analysis of variance (RM-ANOVA). The factors were laser type (Nd:YAP/CO_2), skin (dorsum/palm) and intensity (low and high). Sphericity was investigated, but according to Mauchly test of sphericity, the sphericity assumption was violated for both the RT and NRS data, thus, the Huynh–Feldt correction was applied.

The LEP amplitude and latencies were analysed using two separate RM-ANOVAs. For the N2P2 amplitude, a three-way RM-ANOVA was used with factors set as laser type, skin type and stimulation intensity. Since no N1 LEPs were observed when stimulating the palm (see Results section), a two-way ANOVA was used to investigate the N1 data with factors set as laser type and stimulation intensity. For N2, P2 and N1, the Mauchly test showed that assumption of sphericity was violated, thus, the Huynh–Feldt correlation was applied.

The RM-ANOVA analysis was made in SPSS 27 (IBM).

To compare the computational model with the experimental data, a Pearson correlation analysis was made between LEP amplitude (N2P2) and the maximum DEJ temperature as well as between LEP amplitude (N2P2) and the tissue volume above Aδ threshold (46°C) (Frahm et al., 2020). The correlation analysis was made in Matlab R2021a (Mathworks).

For all analysis, *p*-values of less than 0.05 were considered significant.

3 | RESULTS

3.1 | Laser-evoked potentials

The LEPs elicited by Nd:YAP and CO_2 laser stimuli were comparable for stimulation of the hairy skin on the hand dorsum (Figures 1 and 2). For stimuli to the glabrous skin in the palm, Nd:YAP stimuli showed reduced responses compared to the dorsum (Figure 1), whereas CO_2 laser stimuli showed barely present responses in the palm.

Overall, the results show that the N2P2 complex was more robust (Figure 1) than the N1 peak and exhibited larger amplitude than N1 (Table 2).

The N1 amplitudes (Figure 1, Table 2) were significantly dependent on the laser type (RM-ANOVA, *F*(12,

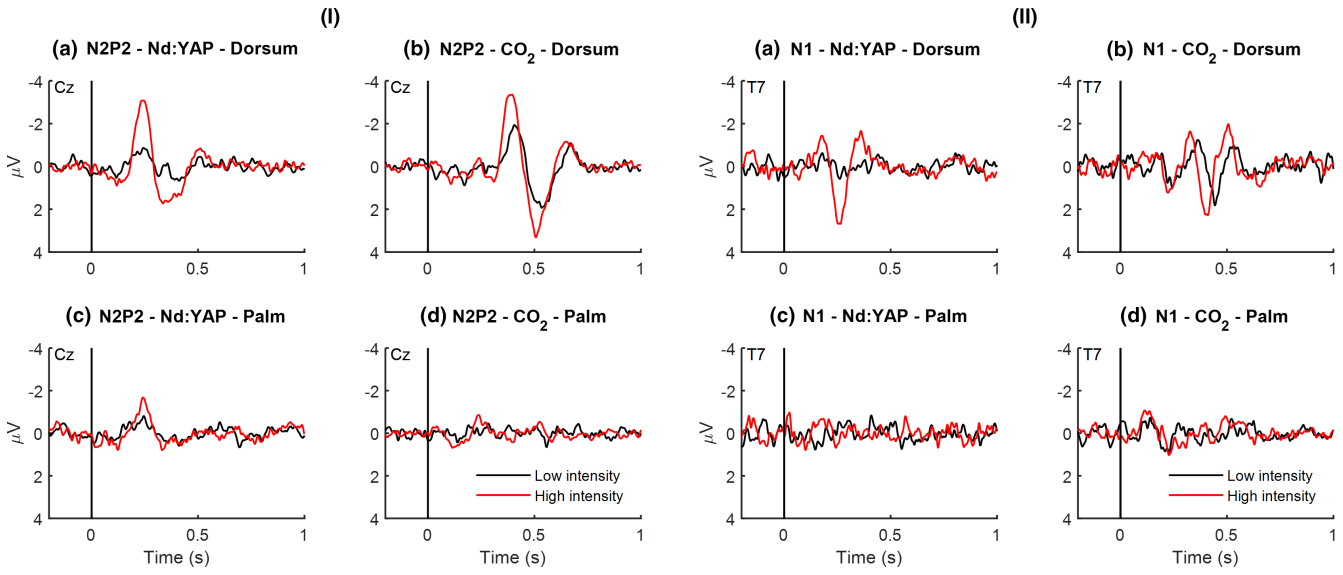

FIGURE 1 Grand average laser-evoked potentials. (I) N2P2 (Cz)—the N2P2 was not significantly dependent on laser type. There was significant interaction in the N2P2 amplitude between laser types and intensity (RM-ANOVA, $F(12, 1) = 5.3$, $p < 0.05$), but also between laser type and skin and between skin and intensity (RM-ANOVA, $F(12, 1) = 14.0$, $p < 0.01$). The vertical line in 0 s indicates stimulation onset. (II) N1 (T7)—the N1 amplitude was significantly dependent on laser type (RM-ANOVA, $F(12, 1) = 6.1$, $p < 0.05$) and intensity (RM-ANOVA, $F(12, 1) = 9.3$, $p < 0.05$). The vertical line in 0 s indicates stimulation onset. For N1 the statistical analysis was only made for hand dorsum stimulation, due to the low amplitude of the response for palm stimulation. (a) Nd:YAP laser stimuli in the hand dorsum, (b) CO_2 laser stimuli in the hand dorsum, (c) Nd:YAP laser stimuli in the palm, (d) CO_2 laser stimuli in the palm.

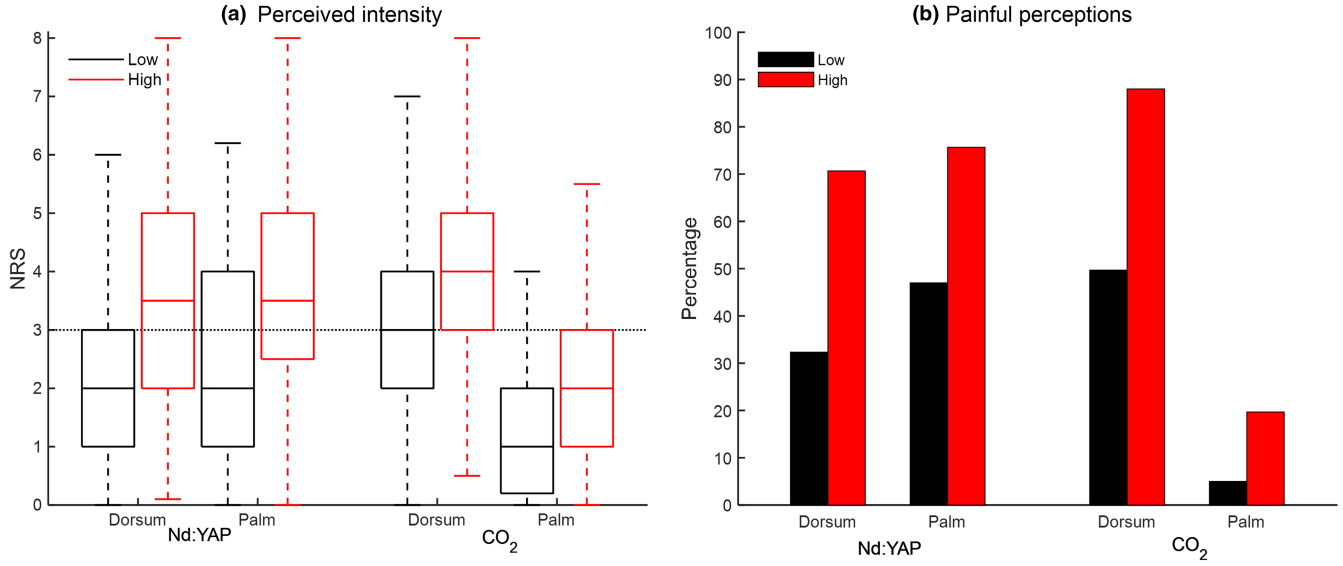

FIGURE 2 Perceived intensities and number of painful perceptions for different laser type (Nd:YAP/CO_2), skin location (dorsum/palm) and intensity (Low, High). (a) Perceived intensity (NRS) boxplot, the box indicates the 25th and 75th quartiles, the horizontal line indicates the median, error bars indicate the 5th and 95th quartiles. There was an interaction between laser type and skin site (RM-ANOVA, $F(12, 1) = 29.6$, $p < 0.001$), and between laser and intensity (RM-ANOVA, $F(12, 1) = 6.8$, $p < 0.05$). CO_2 stimuli in the palm was perceived significantly lower. The NRS was anchored as 0: perception, 3: pain threshold, 10: maximum imaginable pain. (b) Overall percentage of painful perceptions. The majority of the high-intensity stimuli were perceived as painful, except for CO_2 stimuli in the palm.

TABLE 2 Grand average N2P2 and N1 amplitudes of the laser-evoked potentials (mean ± SD).

	N2P2		N1	
	Low intensity	High intensity	Low intensity	High intensity
Nd:YAP – Dorsum	3.7 ± 2.5 μV	7.7 ± 5.1 μV	2.0 ± 1.1 μV	3.0 ± 1.6 μV
CO_2 – Dorsum	6.3 ± 4.3 μV	8.4 ± 4.5 μV	2.9 ± 4.3 μV	3.7 ± 1.7 μV
Nd:YAP – Palm	3.9 ± 1.5 μV	5.3 ± 3.0 μV	N/A	N/A
CO_2 – Palm	2.6 ± 1.4 μV	3.0 ± 1.2 μV	N/A	N/A

Note: The N2P2 amplitude was not significantly dependent on laser type. The N1 amplitude was significantly dependent on both laser type (RM-ANOVA, $F(12, 1) = 6.1$, $p < 0.05$) and intensity (RM-ANOVA, $F(12, 1) = 9.3$, $p < 0.05$). For the N2P2 amplitude, there was a significant interaction between the laser type and intensity (RM-ANOVA, $F(12, 1) = 5.3$, $p < 0.05$), but also between laser type and skin like there was an interaction between skin and intensity (RM-ANOVA, $F(12, 1) = 14.0$, $p < 0.01$). Only N1 data for dorsum were analysed due to no LEP being observed following stimulation of the palm (Figure 1).

1) = 6.1, $p < 0.05$) and the intensity (RM-ANOVA, $F(12$, 1) = 9.3, $p < 0.05$).

For the N2P2 amplitude (Figure 1, Table 2), there was a significant interaction between laser type and stimulation intensity (RM-ANOVA, $F(12, 1) = 5.3$, $p < 0.05$), likely caused by the fact that higher intensity CO_2 stimuli in the palm did not create an increase in LEP amplitude as it is the case for other combinations of laser types and skin types. A significant interaction was also observed between laser type and skin type (RM-ANOVA, $F(12, 1) = 14.0$, $p < 0.05$) likely caused by the barely present CO_2 LEPs when stimulating the palm.

The analysis of the LEP latencies showed that the N1 peak (RM-ANOVA, $F(12, 1) = 70.5$, $p < 0.001$), N2 peak (RM-ANOVA, $F(12, 1) = 505.3$, $p < 0.001$) and P2 peak (RM-ANOVA, $F(12, 1) = 99.7$, $p < 0.001$) were all significantly depending on laser type (Table 3), where CO_2 laser stimuli resulted in significantly delayed LEP component latencies. However, there were no significant effect of other parameters.

3.2 | Perceptual characteristics

The perceived intensity reported by the subjects was significantly dependent on the combination of laser type, skin site and intensity (Figure 2a). There was an interaction between laser type and skin site (Figure 3a,

TABLE 3 Latencies of N2, P2 and N1 peaks during low and high intensities (mean ± SD).

	Low intensity			High intensity		
	N2	P2	N1	N2	P2	N1
Nd:YAP – Dorsum	233 ± 66 ms	399 ± 64 ms	207 ± 43 ms	246 ± 35 ms	387 ± 56 ms	195 ± 39 ms
CO_2 – Dorsum	431 ± 41 ms	535 ± 34 ms	400 ± 66 ms	400 ± 22 ms	508 ± 19 ms	380 ± 66 ms
Nd:YAP – Palm	241 ± 56 ms	391 ± 94 ms	N/A	249 ± 56 ms	368 ± 70 ms	N/A
CO_2 – Palm	414 ± 53 ms	539 ± 60 ms	N/A	447 ± 70 ms	555 ± 73 ms	N/A

Note: For N1, N2 and P2 the latencies were significantly longer for CO_2 laser stimuli (RM-ANOVA, $p < 0.001$).

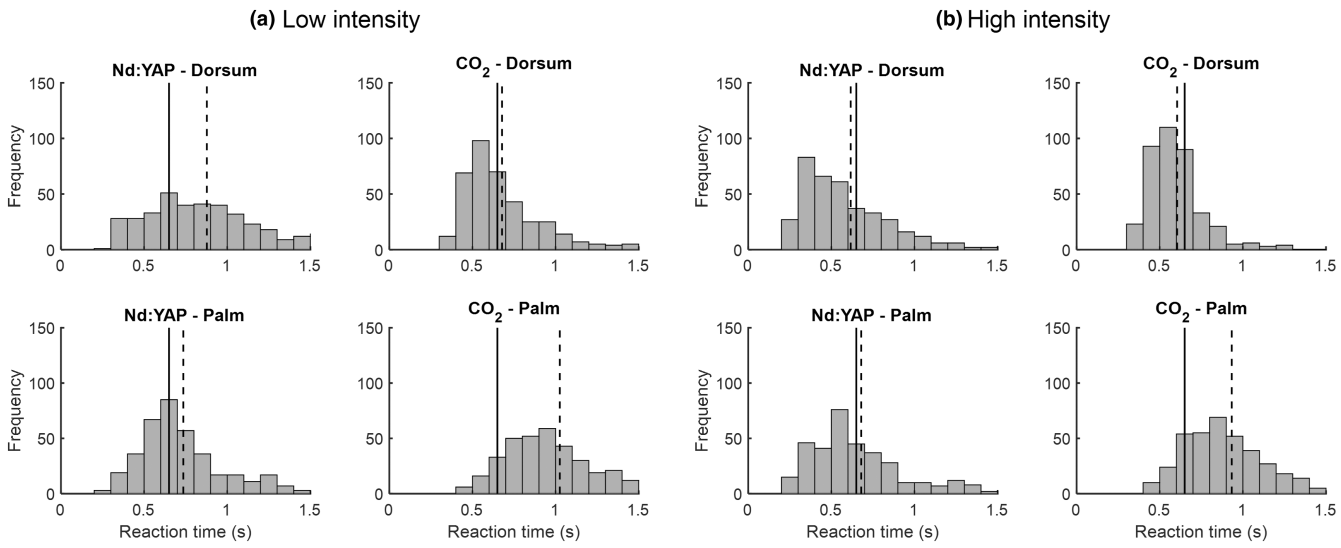

FIGURE 3 Reaction times (a) low intensity, (b) high intensity. Each plot depicts the reaction times of each combination of laser type (Nd:YAP/CO_2) and skin site (dorsum/palm). The vertical full line indicates a 650 ms cut-off between Aδ and C fibre-mediated responses. The vertical dashed line indicates the mean of the reaction times in each condition. There was a significant difference in reaction times between laser types (RM-ANOVA, $F(12, 1) = 6.6$, $p < 0.05$), skin types (RM-ANOVA, $F(12, 1) = 59.0$, $p < 0.001$) and intensity (RM-ANOVA, $F(12, 1) = 7.5$, $p < 0.05$).

RM-ANOVA, $F(12, 1) = 29.6$, $p < 0.001$), and between laser type and intensity (Figure 2a, RM-ANOVA, $F(12, 1) = 6.8$, $p < 0.05$). CO_2 laser stimuli to the palm were perceived significantly lower than other combinations. Unsurprisingly, higher intensities resulted in higher NRS. At the hand dorsum, the perceived intensity for the low intensity was significantly higher for the CO_2 stimuli compared to the Nd:YAP stimuli (RM-ANOVA, $F(12, 1) = 4.8$, $p < 0.05$).

The majority of the high-intensity stimuli were perceived as painful, except for CO_2 stimulation of the palm (Figure 2b). For the lower intensity, approximately half of the stimuli were perceived as painful, however, for CO_2 stimuli delivered to the palm, this was less than 20% (Figure 2b).

The reaction times for CO_2 stimulation of the palm were significantly longer than other combinations of skin location and laser type. Higher intensities generally resulted in shorter reaction times (Figure 3b). The reaction times to the laser stimulation showed a significant interaction between laser type and skin type (Figure 3, RM-ANOVA, $F(12, 1) = 44.2$, $p < 0.001$). There was a significant difference in reaction times between laser types (RM-ANOVA, $F(12, 1) = 6.6$, $p < 0.05$), skin types (RM-ANOVA, $F(12, 1) = 59.0$, $p < 0.001$) and intensity (RM-ANOVA, $F(12, 1) = 7.5$, $p < 0.05$).

3.3 | Computational results

3.3.1 | Model versus LEPs

Our previous validated computational model was used to investigate the dependency of LEP parameters on the stimulation characteristics (laser type, skin location and intensity). Since the N1 data were less robust compared to the N2P2, only the N2P2 amplitude was compared to the model. The comparison between the computational model and the LEP data showed a good agreement between the simulated nociceptor temperature and LEP

(Figure 5b vs. c). Interestingly, the model showed little agreement between the skin surface temperature and the LEP amplitude (Figures 5a vs. c and 6c).

There was a significant correlation between the LEP amplitude (N2P2) and the maximum temperature at the DEJ (Figure 5a, Pearson, $p < 0.01$, $r = 0.92$). Moreover, there was a significant correlation between LEP amplitude (N2P2) and tissue volume above 46°C but with a lower correlation coefficient (Figure 5b, Pearson, $p < 0.05$, $r = 0.80$).

3.3.2 | Simulation of Nd:YAP And CO_2 stimulation characteristics

The computational model was also used to compare Nd:YAP and CO_2 stimuli of similar duration (20 ms). Shorter CO_2 stimuli with a similar surface temperature as used in this study would result in a lower nociceptor temperature (Figure 6c), likely to be below Aδ threshold. Obtaining a nociceptor temperature like the CO_2 stimuli used experimentally would entail reaching a skin surface temperature of more than 65°C (Figure 6d) in hairy skin. In glabrous skin, the differences for shorter CO_2 stimuli were exacerbated (Figure 6g,h) to reach a similar DEJ temperature during a 20 ms would require a surface temperature in excess of 80°C.

Stimulation with a Nd:YAP laser entails a larger distribution of the laser energy and thus requires little or no thermal conduction in the skin before the nociceptors can be activated (Figure 6). The larger penetration of the Nd:YAP gives a lower thermal gradient in the tissue, resulting in slower cooling after stimulation offset (Figure 7). The computational model showed that the tissue temperature remains above Aδ nociceptor threshold (46°C) for approx. 1 s after stimulation offset during Nd:YAP stimuli (Figure 7).

4 | DISCUSSION

This study investigated the laser-evoked potentials elicited by stimulation of both hairy and glabrous skin using Nd:YAP and CO_2 lasers. The results show that while LEPs are reliably elicited in the hairy skin using either laser type, the LEPs and the perceived intensities following CO_2 laser stimulation in glabrous skin are significantly reduced relative to other combinations of laser and skin type. These differences were investigated using a previously validated computational model. The model demonstrated that, whereas Nd:YAP elicits a similar nociception activation irrespective of skin type, the low-penetrance CO_2 laser stimuli activate less nociceptors in glabrous skin. The model predicted that the thicker glabrous skin prevents the thermal energy from the CO_2 laser stimulus from bringing nociceptors to a temperature exceeding their thermal activation threshold.

4.1 | Laser-evoked potentials—dependence on stimulation characteristics

Similar to Perchet et al., we found reproducible LEPs for both CO_2 and Nd:YAP laser stimuli in hairy skin (Perchet et al., 2008). Additionally, we showed that the laser-evoked potentials following cutaneous laser stimulation depend on the laser wavelength, skin type and stimulation intensity (Figures 1 and 2). The computational modelling showed that the thinner hairy skin, with more superficially terminating nociceptors, as found in the hand dorsum, can be similarly activated by CO_2 and Nd:YAP stimuli, which supports the experimental findings. Generally, we found that the nociceptor activation simulated by the model (maximum receptor temperature and activated tissue volume) were both highly predictive of the experimental LEP amplitudes (Figure 5), however, the best prediction was found for the maximum receptor temperature at the dermo-epidermal junction (DEJ). The DEJ temperature indicates that both laser types are capable of activating A fibre hand dorsum, while only the Nd:YAP laser stimuli are capable of activating these receptors in the hand palm. In the thicker glabrous skin, the nociceptors terminate deeper (Frahm et al., 2010), meaning that the energy from a low penetrance laser stimulus, like a CO_2 laser stimulus, needs to be conducted through a larger distance before reaching the terminals. This passive heat conduction limits the potential nociceptor activation. Additionally, the thicker epidermal layers in glabrous skin (Frahm et al., 2010) also reduces the conduction of the thermal energy into the skin due to higher thermal insulation. Overall, these characteristics create higher surface temperatures for CO_2 stimuli in the palm, but lower nociceptor temperatures (Figure 4). The latter reduces the afferent volley affecting the evoked potentials (Figures 1 and 2), the perceived intensity (Figure 2) and the reaction times (Figure 3). On the other hand, the Nd:YAP laser penetrates deeper into the skin, meaning that a greater fraction of the thermal energy is absorbed at nociceptor level, reducing the thermal conduction needed for nociceptor activation. This was reflected by the LEPs elicited by Nd:YAP stimuli in the palm, which were larger than those elicited by CO_2 stimuli in the palm. The computational results support these findings and indicate the underlying reason behind the reduced LEPs from glabrous skin following CO_2 laser stimuli (Figure 4). Similar to CO_2 laser stimuli, contact-heat stimuli using thermodes to create a very superficial heating of the skin

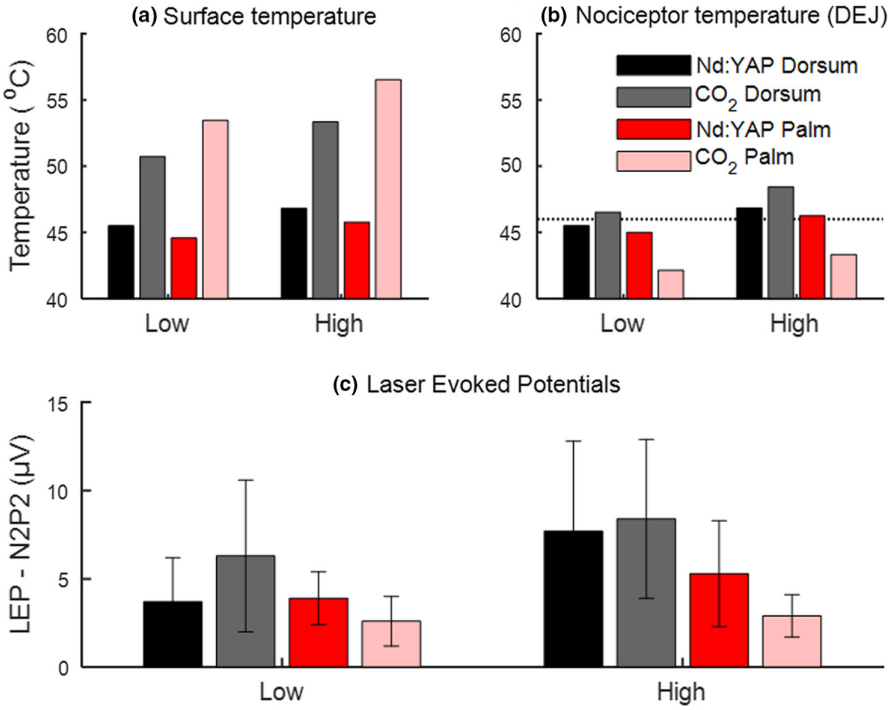

FIGURE 4 Comparison between the simulated (a) surface temperatures and (b) nociceptor temperature at the DEJ and (c) recorded LEP (N2P2) amplitudes. The figure depicts all combinations of laser type (Nd:YAP/CO_2), skin (dorsum/palm) and intensity (Low, High). The horizontal dashed line in (b) indicate 46°C—equivalent to Aδ nociceptor threshold. It is worth noting how the CO_2 stimuli in the palm results in the highest surface temperatures, but in contrast show the lowest nociceptor temperature and give the lowest LEP amplitude.

that requires passive heat conduction to reach the nociceptors. Contact heat-evoked potentials (CHEPS) in the glabrous skin of the palm have been shown to elicit smaller evoked responses than those elicited from the hairy skin (Iannetti et al., 2006), further demonstrating the insulation effect caused by the thicker skin. Like the current study, Iannetti et al. showed that Nd:YAP elicits comparable LEPs, irrespective of skin type. A recent study comparing laser stimuli across skin types also reported a lower degree of nociceptor activation following CO_2 laser stimuli in glabrous skin (Lefaucheur et al., 2021). The authors reported that CO_2 stimuli in glabrous skin only elicited responses associated with C fibre nociceptors, not Aδ nociceptors, indicating a lower receptor temperature, insufficient to activate the thermosensitive Aδ nociceptors, which have higher thermal thresholds than C fibres (Churyukanov et al., 2012; Treede et al., 1995).

The experimental data in this study, both electrophysiological (LEPs) and behavioural (NRS and RT), indicate that the responses seen in the palm following Nd:YAP stimulation are in accordance with A fibre-mediated responses, especially for the higher stimulation intensity. This finding is in agreement with Iannetti et al. (2006) also showing A fibre responses from the glabrous skin following Nd:YAP stimulation, thus, further demonstrating that A type II nociceptive fibres are in fact also present in the palm, and not limited to only hairy skin as previously suggested by Treede et al. (1995). At the hand dorsum, the responses following both Nd:YAP and CO_2 laser stimuli are also in accordance with A fibre-mediated responses, in particular for the highest stimulation intensity.

The stimulation duration of the laser stimuli differed between the two laser types in this study. While shorter CO_2 stimuli are technically feasible, such durations are likely to cause skin erythema (Perchet et al., 2008). For shorter duration CO_2 laser stimuli, the power output must be increased to allow sufficient temperature increases at nociceptor level, which increases the risk of skin damages and erythema (Figure 6). However, longer stimulus duration can lead to a less synchronized afferent signal, and it is likely to affect the LEPs (Iannetti et al., 2004). It is therefore possible that the combination of longer pulse duration and thermal insulation of the CO_2 stimuli have further exacerbated the reduced LEP amplitude observed in the palm, resulting in the difficulty of eliciting LEPs from the palm using CO_2 laser stimuli. Overall, it can also be noted that the LEP amplitudes observed in this study are lower than what has been reported in other studies (Truini et al., 2005). However, this may again be explained by the longer pulse duration of both lasers. Longer pulse durations have been shown to increase LEP latencies and decrease amplitude, particularly for the N1 potential (Iannetti et al., 2004), which is in agreement with the results found in this study. Originally, these durations were chosen to optimally validate the computational model (Frahm et al., 2020). However, the effect and potential disadvantages of shorter CO_2 durations were shown using the computational model (Figure 6).

The differences in the N2P2 complex between different combinations of laser and skin types (Figure 1, Table 2) can be explained by the biophysical characteristics of the

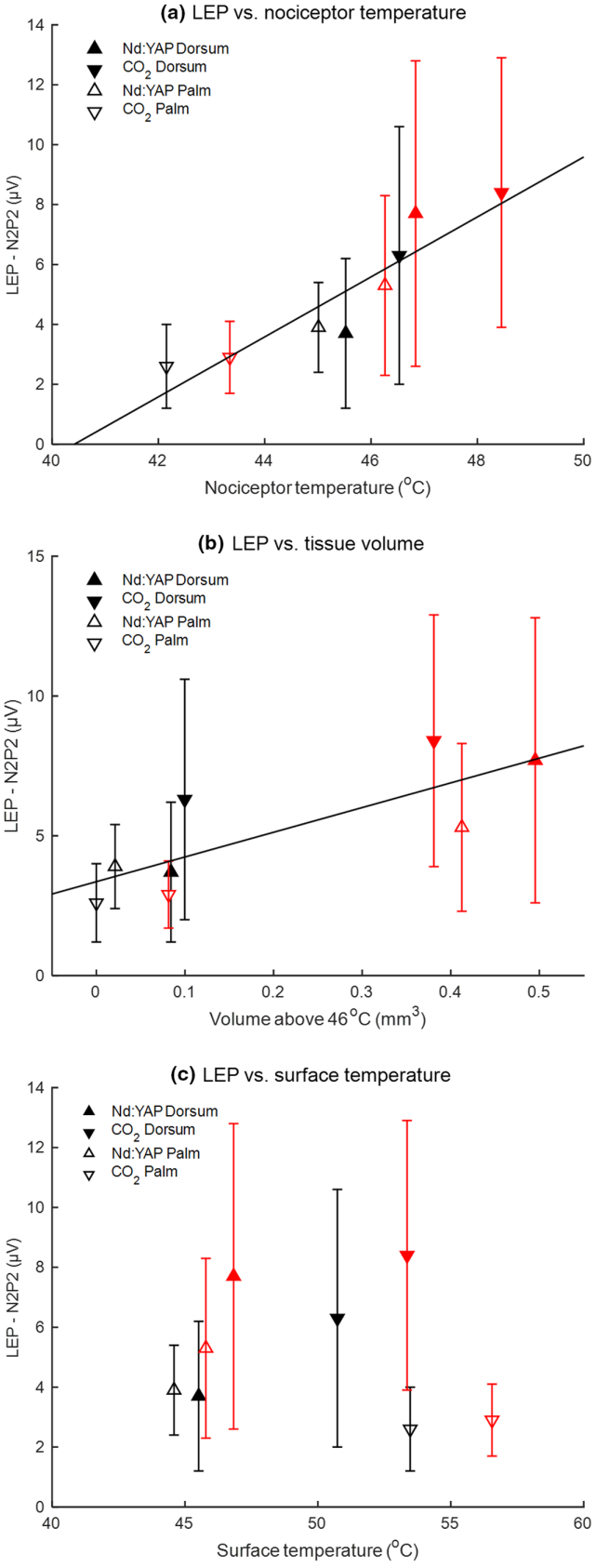

FIGURE 5 Correlation between LEP amplitudes (N2P2), indicated as mean ± SD, and (a) the simulated maximum temperature at the DEJ of the simulated tissue, (b) the simulated tissue volume above Aδ threshold (≥46°C) and (c) the simulated maximum surface temperature. There was a significant correlation for both (a) and (b), but not (c). (a) The black line indicates the linear correlation between LEP amplitude and nociceptor temperature ($p < 0.01$, $r = 0.92$). (b) The black line indicates the correlation between LEP amplitude and tissue volume above threshold ($p < 0.05$, $r = 0.80$). (c) A linear regression analysis between LEP amplitude and skin surface temperature showed no significant relationship ($p = 0.80$, $r = -0.11$), indicating that skin surface temperature is not a good predictor of LEP amplitude. Colours refer to stimulation intensity (black: low intensity, red: high intensity).

skin and laser absorption. Nonetheless, it is surprising to see that stimulation of the glabrous skin did not elicit any detectable N1 potentials (Figure 1, Table 2). Previously, Nd:YAP stimulation of the palm was shown to elicit reliable N1 potentials, though with smaller amplitudes than in hairy skin (Iannetti et al., 2006). One important difference that may reduce the Nd:YAP N1 potential from the glabrous skin could be the longer Nd:YAP stimulation duration (20 ms in the present study compared to 4 ms used in previous studies) (Iannetti et al., 2006). In fact, the N1 amplitude has been shown to be reduced for longer stimulus durations (Iannetti et al., 2004). Additionally, it is generally agreed that the N1 potentials are more difficult to elicit (Iannetti et al., 2006; Truini et al., 2005), and thus many LEP studies only report the N2P2 complex.

4.2 | Thermal energy distribution after cutaneous laser stimuli

As discussed above, the deeper penetration of Nd:YAP laser stimuli allows a very direct nociceptor activation without the need for heat conduction as correctly speculated by (Iannetti et al., 2004; Perchet et al., 2008), and as also supported by our computational model (Frahm et al., 2020). However, this deeper penetrance of Nd:YAP laser stimuli heats a tissue volume which has a dramatically different shape compared to that following CO_2 stimulation. Due to the circular laser beam, the tissue volume which is heated by the stimulus will be shaped as a cylinder (Frahm et al., 2020; Leandri et al., 2006). While the absorption of a CO_2 laser stimulus resembles a disk constrained to the surface of the skin, the distribution after Nd:YAP stimulation resembles a cylinder extending deep within the skin (Frahm et al., 2020). The larger distribution following Nd:YAP stimulation will result in a lower temperature gradient as a function of depth, which is likely to lead to a prolonged cooling phase.

Similar to Leandri et al. (2006), our model demonstrates how the Nd:YAP cooling period is much longer than the one following CO_2 stimuli (Figure 7). This must be taken into consideration during Nd:YAP laser

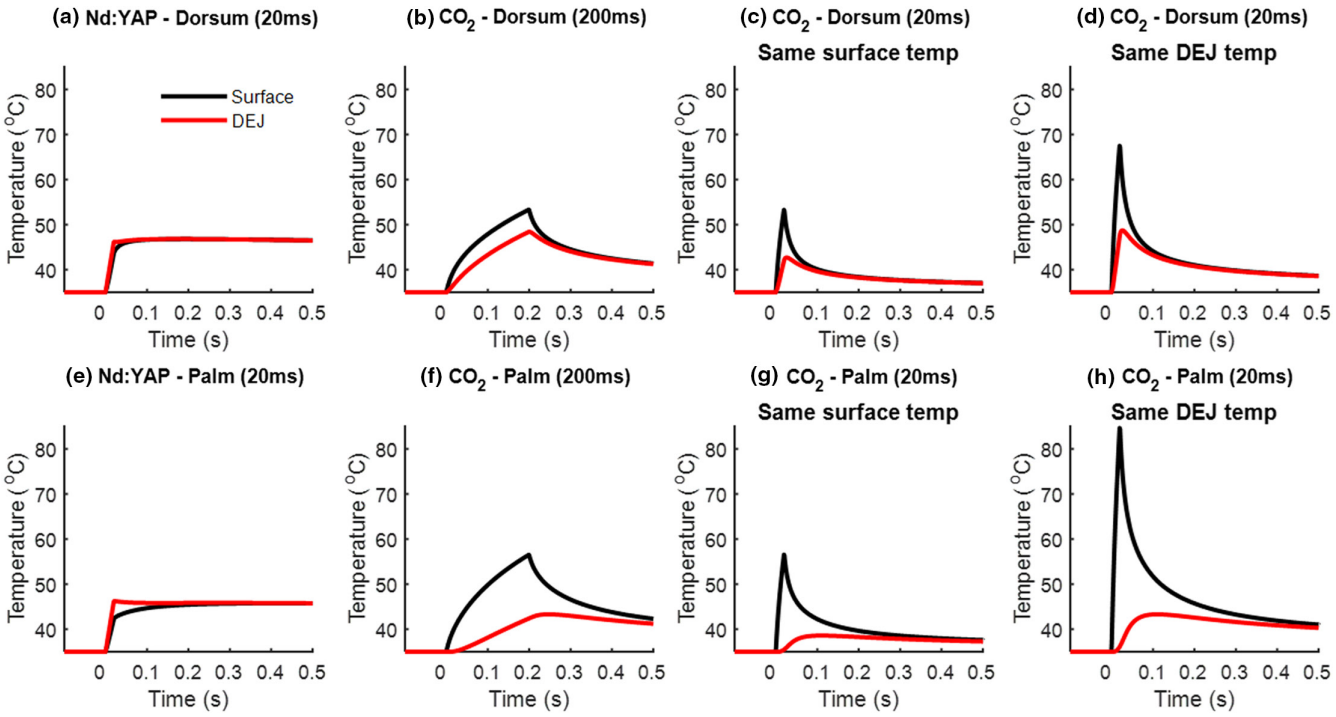

FIGURE 6 Computational comparison of Nd:YAP and CO_2 stimuli of similar duration (high intensity) in both the dorsum (a–d) and palm (e–h) of the hand. (a, b, e, f) Simulated surface and DEJ temperature profiles of Nd:YAP and CO_2 laser stimulation used experimentally (Nd:YAP duration 20 ms, CO_2 duration 200 ms) in the dorsum and palm respectively. (c, d, g, h) Simulated temperature surface and DEJ to reach same surface temperature (c, g) and to reach same DEJ temperature (d, h), in the dorsum and palm respectively. Notice in (c) how the DEJ temperature is likely below Aδ threshold, even though the skin surface reaches the same temperature as in (b). This is caused by the low penetrance of the CO_2 laser. This effect is further exacerbated for (g) vs. (f) due to the thicker glabrous skin in the palm.

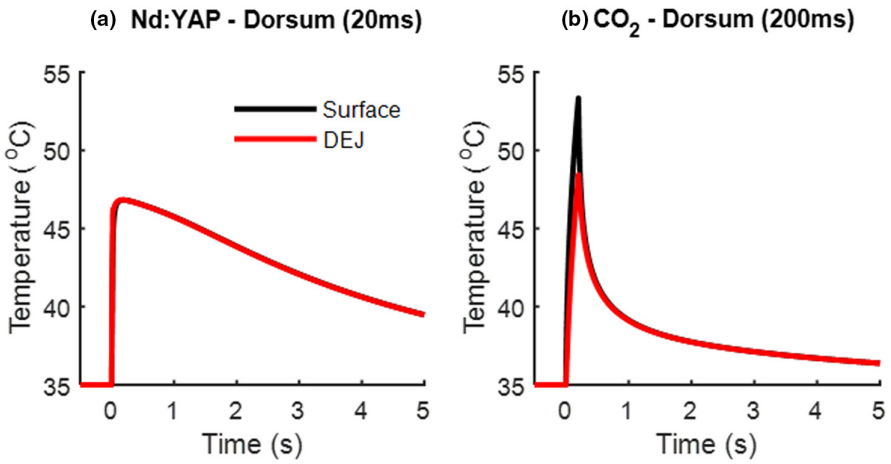

FIGURE 7 Simulation of cooling phase following Nd:YAP (a) and CO_2 (b) laser stimulation (high intensity). Due to higher penetrance of the Nd:YAP laser, the energy is distributed in a larger tissue volume resulting in a prolonged cooling phase compared to CO_2 stimulation. Such a slow cooling could result in a larger degree of habituation or adaption during Nd:YAP stimuli.

stimulation, and it would be advisable to have longer inter-stimulus intervals than those required for CO_2 laser stimulation.

4.3 | Limitations

The computational model used in this study was validated for the same stimulation parameters as used experimentally (Frahm et al., 2020). However, the model was not validated for the shorter pulse durations for CO_2 stimulation that were also used in this study. Since the mathematical model was developed and validated across a large variety of different stimulation parameters such as model geometry (skin thickness in relation to hairy and glabrous skin types), stimulation intensity and laser type (wavelength), it is likely that the model provides valid estimates of other stimulation characteristics. Previously, we have developed and validated a similar model approach across different stimulation for CO_2 stimuli (Frahm et al., 2010).

Therefore, it is believed that the additional simulations can still be considered valid.

5 | CONCLUSION

In this study, we showed how laser-evoked potentials depend on the stimulation parameters, such as laser wavelength, skin type and stimulation intensity. These differences were examined using a previously validated computational model. The model showed that the observed experimental differences found in both the psychophysical and LEP data, can largely be attributed to the biophysical properties of the skin and the absorption characteristics of the different laser wavelength. Specifically, it was shown that CO_2 laser stimulation of the glabrous skin of the hand palm is less capable of activating nociceptive receptors, likely because of the thicker skin in the palm and lower CO_2 laser penetrance. Additionally to this, the duration of CO_2 laser stimuli was also longer than that of the Nd:YAP laser stimuli. This longer stimulus duration may have further exacerbated the reduced responses from the palm. The results of this study will likely be relevant for future studies investigating LEPs and show how the stimulus characteristic affect the LEPs.

AUTHOR CONTRIBUTIONS

Ken Steffen Frahm, Sabata Gervasio, Federico Arguissain and André Mouraux conceived and designed the study. Ken Steffen Frahm, Sabata Gervasio and Federico Arguissain performed the experiments. Ken Steffen Frahm, Sabata Gervasio and Federico Arguissain analysed and interpreted the data. Ken Steffen Frahm drafted the manuscript. Ken Steffen Frahm, Sabata Gervasio, Federico Arguissain and André Mouraux revised the manuscript. All authors have read and approved the final version of the manuscript.

ACKNOWLEDGMENTS

This study was supported by the Danish National Research Foundation (DNRF121).

FUNDING INFORMATION

This study was supported by the Danish National Research Foundation (DNRF121).

CONFLICT OF INTEREST STATEMENT

The authors declare no conflict of interest.

ORCID

Ken Steffen Frahm https://orcid.org/0000-0003-0324-3756

Sabata Gervasio https://orcid.org/0000-0001-6649-7150

André Mouraux https://orcid.org/0000-0003-1056-5980

REFERENCES

Bromm, B., & Treede, R.-D. (1983). CO_2 laser radiant heat pulses activate C nociceptors in man. *Pflügers Archive - European Journal of Physciology*, *399*, 155–156.

Chang, C. Y., Hsu, S. H., Pion-Tonachini, L., & Jung, T. P. (2020). Evaluation of artifact subspace reconstruction for automatic artifact components removal in multi-channel EEG recordings. *IEEE Transactions on Biomedical Engineering*, *67*(4), 1114–1121. https://doi.org/10.1109/TBME.2019.2930186

Churyukanov, M., Plaghki, L., Legrain, V., & Mouraux, A. (2012). Thermal detection thresholds of Aδ- and C-fibre afferents activated by brief CO_2 laser pulses applied onto the human hairy skin. *PLoS One*, *7*(4), 1–10. https://doi.org/10.1371/journal.pone.0035817

Cruccu, G., Aminoff, M. J., Curio, G., Guerit, J. M., Kakigi, R., Mauguiere, F., Rossini, P. M., Treede, R. D., & Garcia-Larrea, L. (2008). Recommendations for the clinical use of somatosensory-evoked potentials. *Clinical Neurophysiology*, *119*(8), 1705–1719.

Cruccu, G., Sommer, C., Anand, P., Attal, N., Baron, R., Garcia-Larrea, L., Haanpaa, M., Jensen, T. S., Serra, J., & Treede, R. D. (2010). EFNS guidelines on neuropathic pain assessment: Revised 2009. *European Journal of Neurology*, *17*(8), 1010–1018. https://doi.org/10.1111/j.1468-1331.2010.02969.x

Delorme, A., & Makeig, S. (2004). EEGLAB: An open source toolbox for analysis of single-trial EEG dynamics including independent component analysis. *Journal of Neuroscience Methods*, *134*(1), 9–21. https://doi.org/10.1016/j.jneumeth.2003.10.009

Frahm, K. S., Andersen, O. K., Arendt-Nielsen, L., & Mørch, C. D. (2010). Spatial temperature distribution in human hairy and glabrous skin after infrared CO_2 laser radiation. *Biomedical Engineering Online*, *9*(1), 69. https://doi.org/10.1186/1475-925X-9-69

Frahm, K. S., & Gervasio, S. (2021). The two-point discrimination threshold depends both on the stimulation noxiousness and modality. *Experimental Brain Research*, *239*(5), 1439–1449. https://doi.org/10.1007/s00221-021-06068-x

Frahm, K. S., Gervasio, S., Arguissain, F., & Mouraux, A. (2020). New insights into cutaneous laser stimulation—Dependency on skin and laser type. *Neuroscience*, *448*, 71–84. https://doi.org/10.1016/j.neuroscience.2020.09.021

Frahm, K. S., Mørch, C. D., & Andersen, O. K. (2018). Tempo-spatial discrimination is lower for noxious stimuli than for innocuous stimuli. *Pain*, *159*(2), 393–401.

Garcia-Larrea, L., Frot, M., & Valeriani, M. (2003). Brain generators of laser-evoked potentials: From dipoles to functional significance. *Neurophysiologie Clinique*, *33*(6), 279–292. https://doi.org/10.1016/j.neucli.2003.10.008

Haimi-Cohen, R., Cohen, A., & Carmon, A. (1983). A model for the temperature distribution in skin noxiously stimulated by a brief pulse of CO_2 laser radiation. *Journal of Neuroscience Methods*, *8*(2), 127–137. https://doi.org/10.1016/0165-0270(83)90113-9

Iannetti, G. D., Leandri, M., Truini, A., Zambreanu, L., Cruccu, G., & Tracey, I. (2004). Aδ nociceptor response to laser stimuli: Selective

effect of stimulus duration on skin temperature, brain potentials and pain perception. *Clinical Neurophysiology*, *115*(11), 2629–2637. https://doi.org/10.1016/j.clinph.2004.05.023

Iannetti, G. D., Zambreanu, L., & Tracey, I. (2006). Similar nociceptive afferents mediate psychophysical and electrophysiological responses to heat stimulation of glabrous and hairy skin in humans. *The Journal of physiology*, *1*, 235–248. https://doi.org/10.1113/jphysiol.2006.115675

Jacques, S. L. (1996). Origins of tissue optical properties in the UVA, visible, and NIR regions. OSA TOPS on advances in optical imaging and photon migration, February, 364–371.

Jacques, S. L. (2013). Optical properties of biological tissues: A review. *Physics in Medicine and Biology*, *58*, R37–R61.

La Cesa, S., Di Stefano, G., Leone, C., Pepe, A., Galosi, E., Alu, F., Fasolino, A., Cruccu, G., Valeriani, M., & Truini, A. (2018). Skin denervation does not alter cortical potentials to surface concentric electrode stimulation: A comparison with laser evoked potentials and contact heat evoked potentials. *European Journal of Pain*, *22*(1), 161–169. https://doi.org/10.1002/ejp.1112

Leandri, M., Saturno, M., Spadavecchia, L., Iannetti, G. D., & Cruccu, G. (2006). Measurement of skin temperature after infrared laser. *Neurophysiologie Clinique*, *36*, 207–218. https://doi.org/10.1016/j.neucli.2006.08.004

Lefaucheur, J. P., Abbas, S. A., Lefaucheur-Ménard, I., Rouie, D., Tebbal, D., Bismuth, J., & Nordine, T. (2021). Small nerve fiber selectivity of laser and intraepidermal electrical stimulation: A comparative study between glabrous and hairy skin. *Neurophysiologie Clinique*, *51*(4), 357–374. https://doi.org/10.1016/j.neucli.2021.06.004

Lejeune, N., Petrossova, E., Frahm, K. S., & Mouraux, A. (2023). High-speed heating of the skin using a contact thermode elicits brain responses comparable to CO_2 laser-evoked potentials. *Clinical Neurophysiology*, *146*, 1–9. https://doi.org/10.1016/j.clinph.2022.11.008

Madden, V. J., Kamerman, P. R., Bellan, V., Catley, M. J., Russek, L. N., Camfferman, D., & Moseley, G. L. (2019). Was that painful or nonpainful? The sensation and pain rating scale performs well in the experimental context. *Journal of Pain*, *20*(4), 472.e1–472.e12. https://doi.org/10.1016/j.jpain.2018.10.006

Marchandise, E., Mouraux, A., Plaghki, L., & Henrotte, F. (2014). Finite element analysis of thermal laser skin stimulation for a finer characterization of the nociceptive system. *Journal of Neuroscience Methods*, *223*, 1–10. https://doi.org/10.1016/j.jneumeth.2013.11.010

Meyer, R. A., Walker, R. E., & Mountcastle, V. B., Jr. (1976). A laser stimulator for the study of cutaneous thermal and pain sensations. *IEEE Transactions on Biomedical Engineering*, *23*, 54–60.

Mor, J., & Carmon, A. (1975). Laser emitted radiant heat for pain research. *Pain*, *1*(3), 233–237.

Mørch, C. D., Andersen, O. K., Quevedo, A. S., Arendt-Nielsen, L., & Coghill, R. C. (2010). Exteroceptive aspects of nociception: Insights from graphesthesia and two-point discrimination. *Pain*, *151*(1), 45–52. https://doi.org/10.1016/j.pain.2010.05.016

Mouraux, A., Iannetti, G. D., & Plaghki, L. (2010). Low intensity intra-epidermal electrical stimulation can activate Adelta-nociceptors selectively. *Pain*, *150*, 199–207. https://doi.org/10.1016/j.pain.2010.04.026

Perchet, C., Godinho, F., Mazza, S., Frot, M., Legrain, V., Magnin, M., & Garcia-larrea, L. (2008). Evoked potentials to nociceptive stimuli delivered by CO_2 or Nd:YAP lasers. *Clinical Neurophysiology*, *119*(11), 2615–2622. https://doi.org/10.1016/j.clinph.2008.06.021

Plaghki, L., & Mouraux, A. (2003). How do we selectively activate skin nociceptors with a high power infrared laser? *Neurophysiologie Clinique*, *33*, 269–277. https://doi.org/10.1016/j.neucli.2003.10.003

Treede, R. D., Meyer, R. A., Raja, S. N., & Campbell, J. N. (1995). Evidence for two different heat transduction mechanisms in nociceptive primary afferents innervating monkey skin. *The Journal of Physiology*, *483*(3), 747–758. https://doi.org/10.1113/jphysiol.1995.sp020619

Truini, A., Galeotti, F., Romaniello, A., Virtuoso, M., Iannetti, G. D. D., & Cruccu, G. (2005). Laser-evoked potentials: Normative values. *Clinical Neurophysiology*, *116*(4), 821–826. https://doi.org/10.1016/j.clinph.2004.10.004

Valeriani, M., Pazzaglia, C., Cruccu, G., & Truini, A. (2012). Clinical usefulness of laser evoked potentials. *Neurophysiologie Clinique*, *42*(5), 345–353. https://doi.org/10.1016/j.neucli.2012.05.002

How to cite this article: Frahm, K. S., Gervasio, S., Arguissain, F., & Mouraux, A. (2023). Influence of skin type and laser wavelength on laser-evoked potentials. *European Journal of Pain*, *27*, 1226–1238. https://doi.org/10.1002/ejp.2152